iScience, Volume *25*

Supplemental information

NudC regulated Lis1 stability is essential for the maintenance of dynamic microtubule ends in axon terminals

Dane Kawano, Katherine Pinter, Madison Chlebowski, Ronald S. Petralia, Ya-Xian Wang, Alex V. Nechiporuk, and Catherine M. Drerup

Figure S1

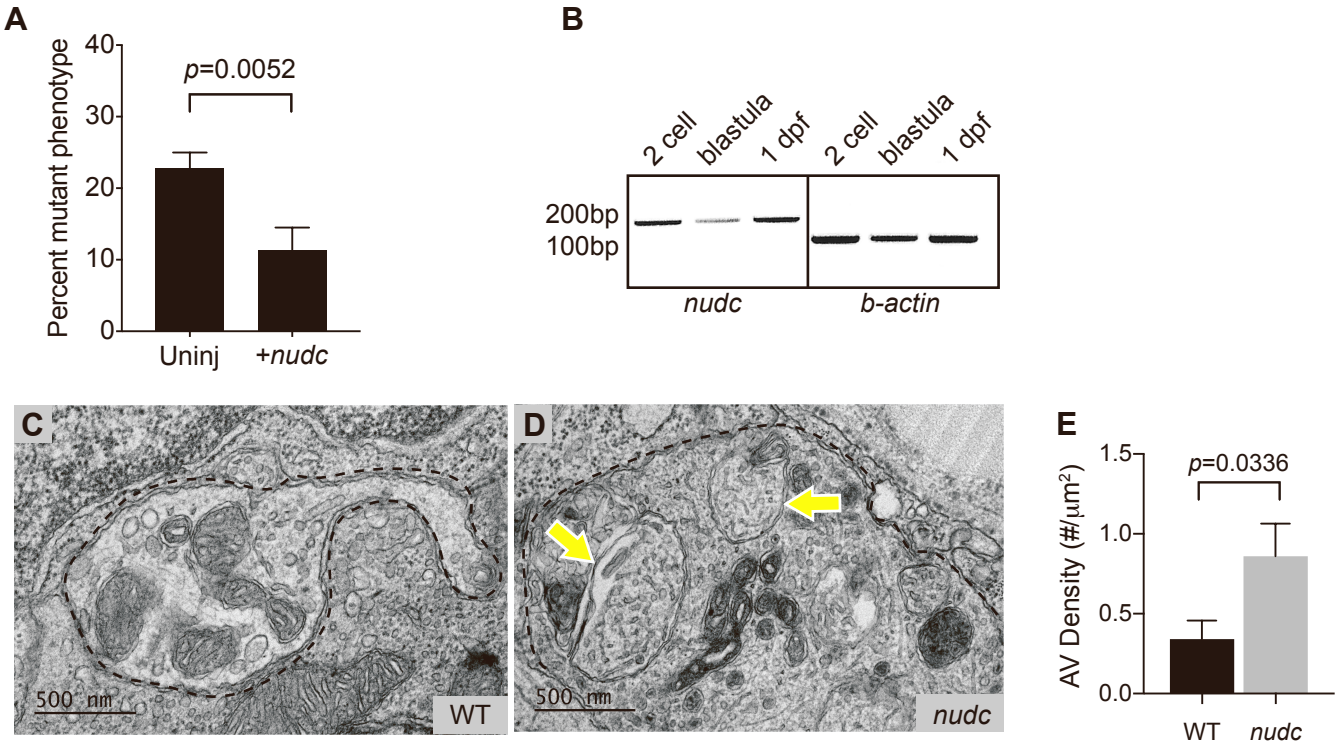

Figure S1. The *nudc* mutation causes loss of NudC function and autophagosome accumulation in axon terminals. Related to Figure 1. (A) Overexpression of mRFP-NudC in nudc mutants can suppress the axon terminal swelling phenotype (ANOVA). Zygotes were injected with mRNA encoding mRFP-NudC for ubiquitous expression in the developing larvae. (B) RT-PCR for nudc shows it is maternally deposited (present at 2-cell stage) and also zygotically expressed. (C,D) Transmission electron micrographs of wild type and *nudc* axon terminals. Enlarged autophagosomes are labeled with yellow arrows. Axon terminal outlined by dashed line. (E) Quantification of autophagosome density in axons from TEM images (ANOVA). Wild type data was collected from 12 micrographs representing 3 fish. *nudc* data was collected from 9 micrographs representing 3 fish. Data are expressed as mean ± S.E.M.

Figure S2

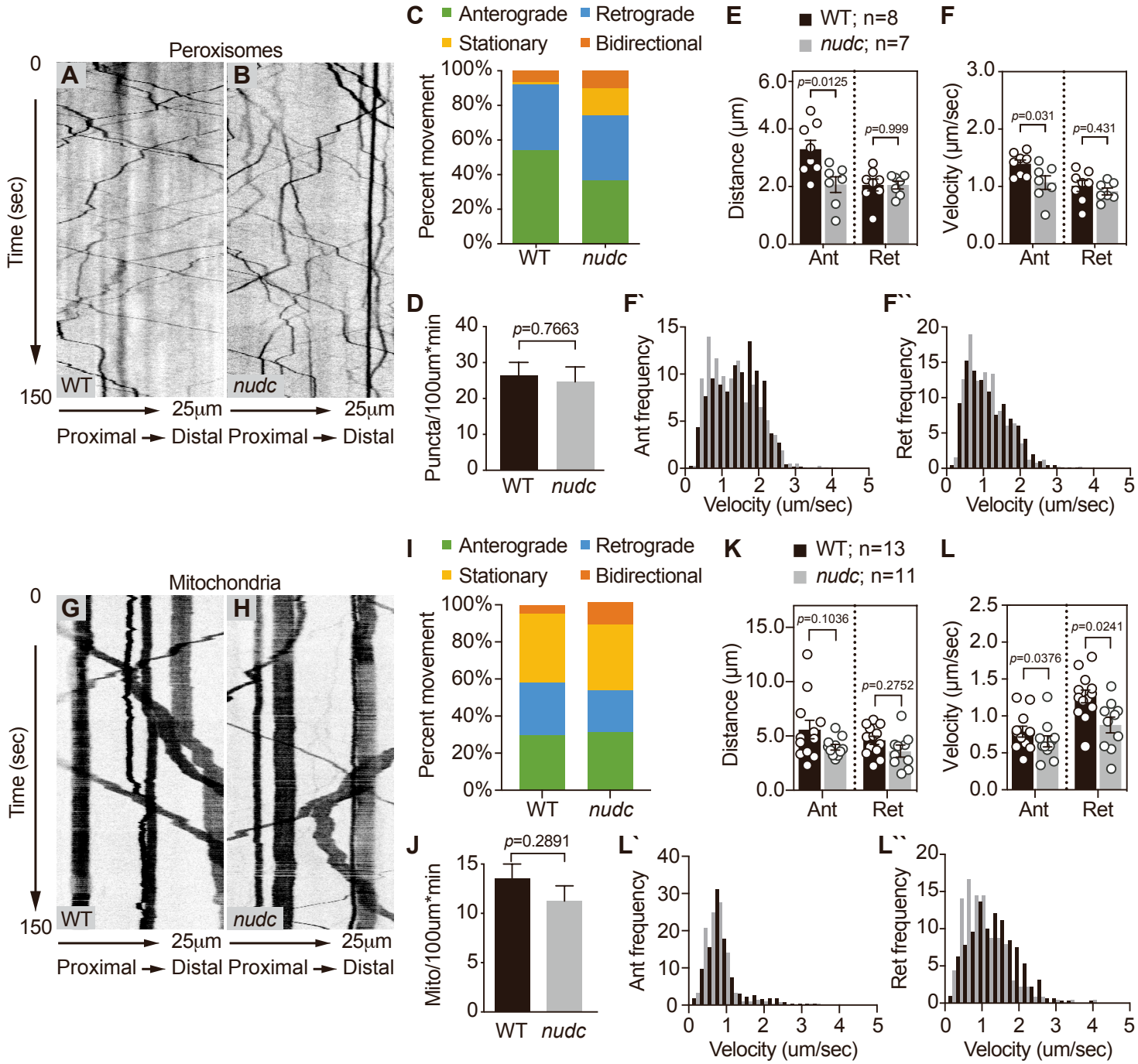

Figure S2. Mitochondrial and peroxisome transport in *nudc* mutants. Related to Figure 2. (A,B) Kymograph analysis of peroxisomes (labeled by a peroxisome targeting sequence tagged with mRFP) transport. (C) Percent of peroxisomes in the anterograde, retrograde, stationary, and bidirectional populations are unaffected in *nudc* mutants. A slight, non-significant reduction in anterograde peroxisome transport was noted (ANOVA; p=0.0553). (D) Total number of peroxisomes present in the axon is unchanged in *nudc* mutants (ANOVA). (E,F) Quantification of peroxisome transport parameters reveals slight decreases in their anterograde distance and velocities in *nudc* mutants (ANOVA). (F`,F``) Histogram of velocities binned in 0.2μm/sec intervals demonstrates a slight shift towards slower anterograde velocities. (G,H) Kymograph analysis of mitochondrial transport. (I) Percent of mitochondria in the anterograde, retrograde, stationary and bidirectional populations are unaffected in *nudc* mutants (ANOVA). (J) Total number of mitochondria present in the axon is unchanged in *nudc* mutants (ANOVA). (K,L) Quantification of mitochondrial transport parameters reveals slight decreases in their anterograde and retrograde transport velocities in *nudc* mutants (Anterograde: Wilcoxon Rank Sum; Retrograde: ANOVA). (L`,L``) Histogram of velocities binned in 0.2μm/sec intervals demonstrates a shift towards slower velocities particularly in the retrograde direction. Data are expressed as mean ± S.E.M. Sample sizes indicated on graph.

Figure S3

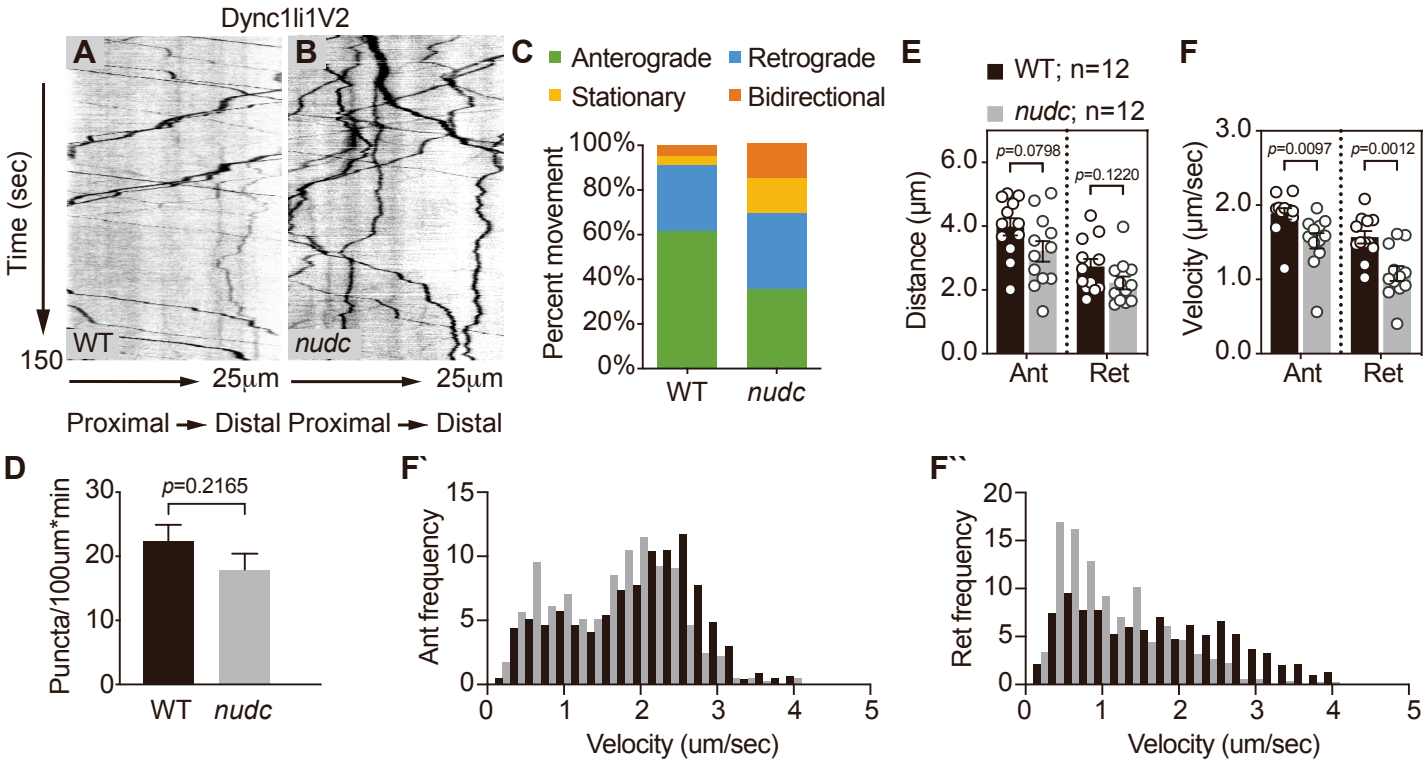

Figure S3. Dync1li1V2-labeled cargo transport in *nudc* mutants. Related to Figure 2. (A,B) Kymograph analysis of Dync1li1v2 transport. (C) The percent of anterograde Dync1li1v2 transport decreases in *nudc* mutants (ANOVA; p=0.0002) while bidirectional movement increases (ANOVA; p=0.0009). Retrograde and stationary Dync1li1V2 punctal transport frequency are unchanged (ANOVA; p=0.3839 and p=0.069 respectively). (D) Total number of Dync1li1V2+ vesicles in the axon are unchanged in *nudc* mutants (ANOVA). (E,F) Quantification of Dync1li1v2 transport shows that anterograde and retrograde velocity are both reduced in *nudc* mutants (ANOVA). (F`F``) Shifts towards slower velocities are clear in the binned histograms. Data are expressed as mean + S.E.M. Sample sizes indicated on graphs.

Figure S4

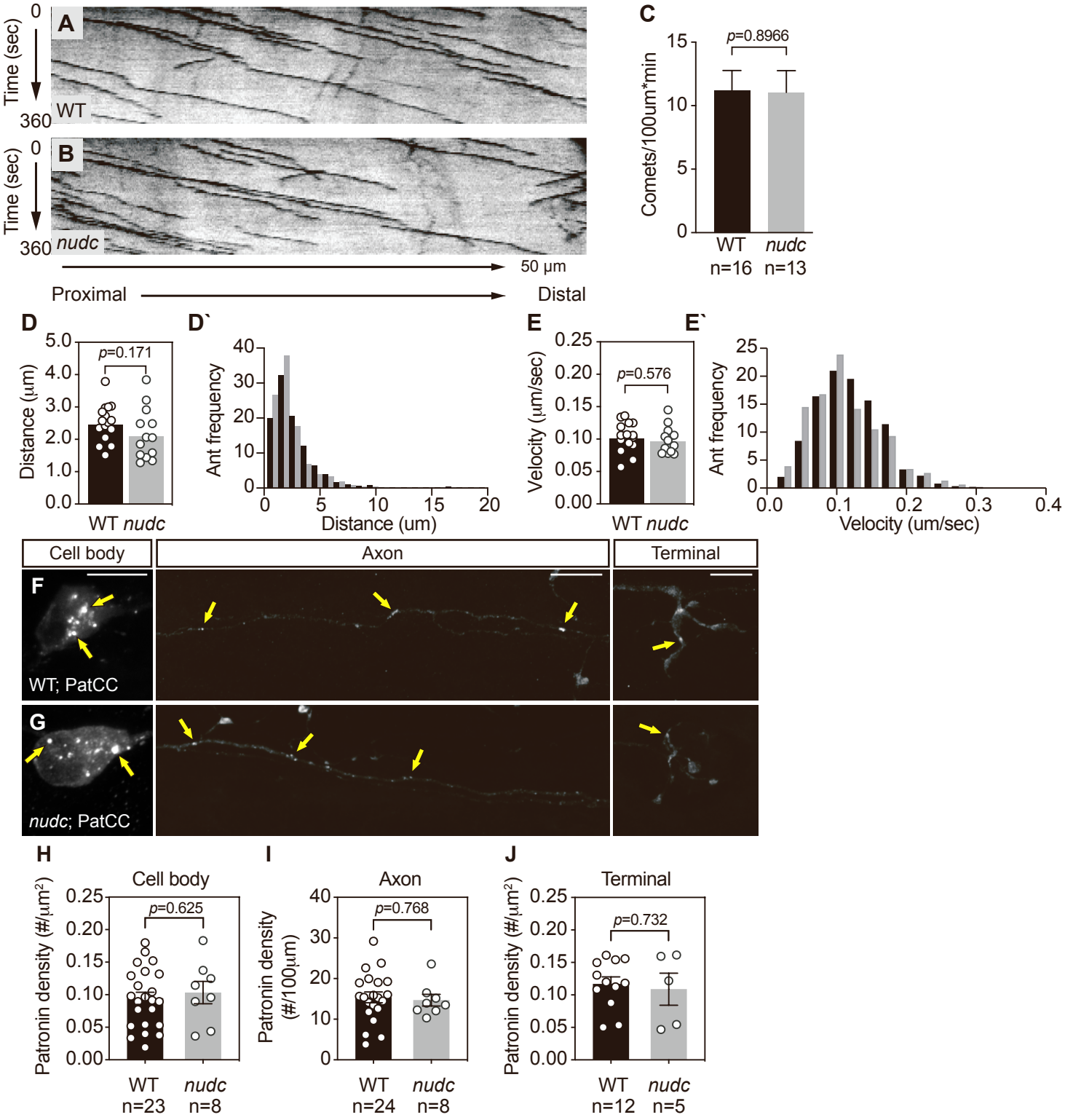

Figure S4. Microtubule stability in the axon shaft is unchanged in *nudc* mutants. Related to Figure 3. (A,B) Kymograph analysis of EB3-labeled microtubule growth. (C) The number of plus-end directed comets are the same between wild type and *nudc* mutants (ANOVA). (D,E) Quantification of microtubule growth distance and velocity show no difference between wild type and *nudc* mutants (ANOVA). (D`, E`) Binned histograms of distance and velocity showing no population shifts for either measurement. (F,G) Images of RFP-Patronin-CC labeling of microtubule minus ends in the cell body, axon, and axon terminal. (H-J) Quantification of Patronin punctal density shows no difference in microtubule minus end number in any compartment (ANOVA). Data are expressed as mean ± S.E.M. Scale bar = 10µm. Sample sizes indicated on graphs.